Science Translational Medicine
AAAS

Supplementary Materials for

Transcobalamin receptor antibodies in autoimmune vitamin B12 central deficiency

John V. Pluvinage *et al.*

Corresponding author: John V. Pluvinage, john.pluvinage@ucsf.edu; Michael R. Wilson, michael.wilson@ucsf.edu

Sci. Transl. Med. **16**, eadl3758 (2024)
DOI: 10.1126/scitranslmed.adl3758

The PDF file includes:

Other Supplementary Material for this manuscript includes the following:

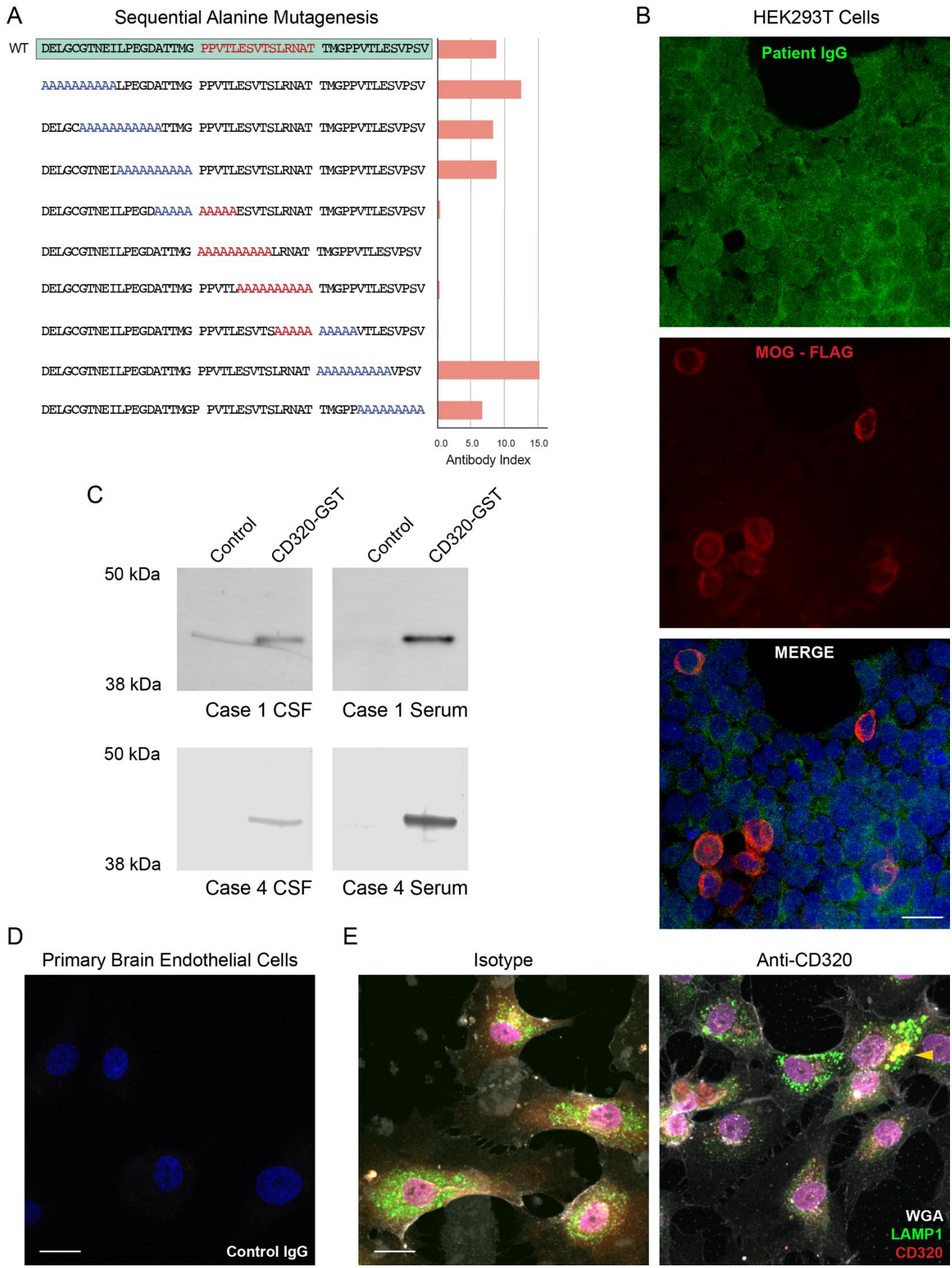
A
Sequential Alanine Mutagenesis
WT DELGCGTNEILPEGDATTMG PPVTLESVTSLRNAT TMGPPVTLESVPSV
AAAAAAAAAALPEGDATTMG PPVTLESVTSLRNAT TMGPPVTLESVPSV
DELGCAAAAAAAAAAATTMG PPVTLESVTSLRNAT TMGPPVTLESVPSV
DELGCGTNEIAAAAAAAAAA PPVTLESVTSLRNAT TMGPPVTLESVPSV
DELGCGTNEILPEGDAAAAA AAAAAESVTSLRNAT TMGPPVTLESVPSV
DELGCGTNEILPEGDATTMG AAAAAAAAAALRNAT TMGPPVTLESVPSV
DELGCGTNEILPEGDATTMG PPVTLAAAAAAAAAA TMGPPVTLESVPSV
DELGCGTNEILPEGDATTMG PPVTLESVTSAAAAA AAAAAVTLESVPSV
DELGCGTNEILPEGDATTMG PPVTLESVTSLRNAT AAAAAAAAAAVPSV
DELGCGTNEILPEGDATTMGP PVTLESVTSLRNAT TMGPPAAAAAAAAA
0.0 5.0 10.0 15.0
Antibody Index
B
HEK293T Cells
Patient IgG
MOG - FLAG
MERGE
C
Control
CD320-GST
Control
CD320-GST
50 kDa
38 kDa
Case 1 CSF
Case 1 Serum
50 kDa
38 kDa
Case 4 CSF
Case 4 Serum
D
Primary Brain Endothelial Cells
Control IgG
E
Isotype
Anti-CD320
WGA
LAMP1
CD320

Fig. S1. Elucidation of anti-CD320 epitope specificity.
(**A**) Ten peptides comprising the CD320 wild-type (WT) sequence (green) or alanine substituted sequences were synthesized and immunoprecipitated with patient CSF antibodies. Antibody index was calculated by comparing the bioluminescence of peptides immunoprecipitated with CSF or protein A/G beads alone. The red sequence (Pro183-Thr197 of NP_057663.1) denotes the antigenic region. (**B**) HEK293T cells were transfected with an irrelevant FLAG-tagged protein (MOG, red) and stained with patient IgG (green) (scale bar = 20 microns). (**C**) Western blot of anti-CD320 antibodies in the CSF and serum of Case 1 (top) and Case 4 (bottom). Recombinant full-length CD320 tagged with glutathione s-transferase (GST) or a truncated version of CD320 lacking the auto-epitope were immunoblotted with patient CSF or serum. (**D**) Immunostaining of primary human brain endothelial cells with healthy control CSF IgG (scale bar = 20 microns). E) Representative images of brain endothelial cells treated with a commercial anti-CD320 antibody and stained for CD320 (red), lysosomes (LAMP1, green), and the plasma membrane (WGA, gray) (scale bar = 20 microns).

A

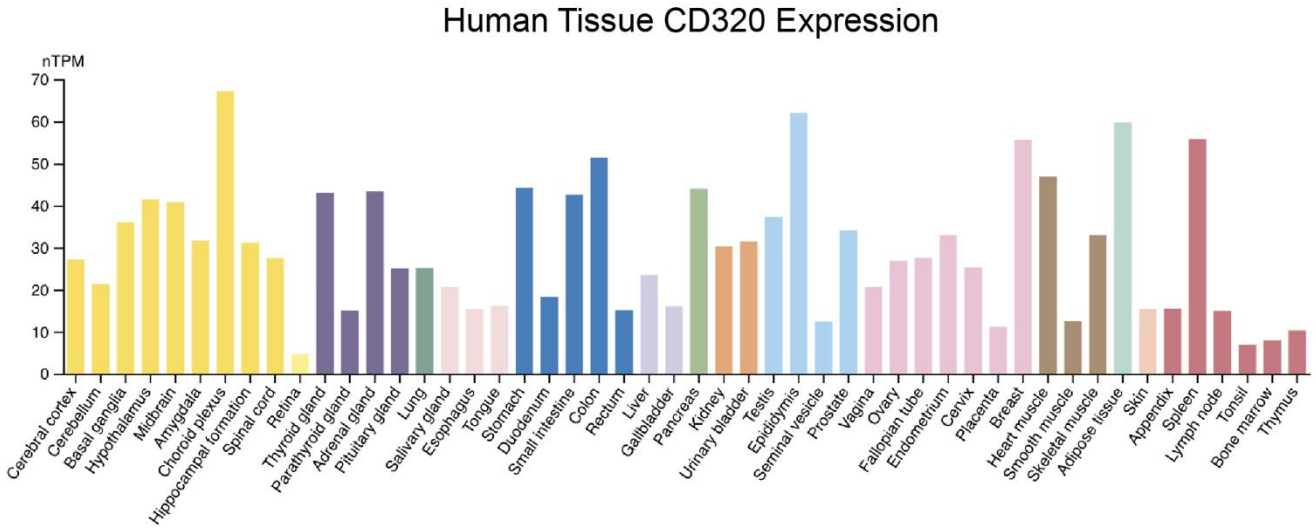
Human Tissue CD320 Expression
nTPM
70
60
50
40
30
20
10
0
Cerebral cortex
Cerebellum
Basal ganglia
Hypothalamus
Midbrain
Amygdala
Choroid plexus
Hippocampal formation
Spinal cord
Retina
Thyroid gland
Parathyroid gland
Adrenal gland
Pituitary gland
Lung
Salivary gland
Esophagus
Tongue
Stomach
Duodenum
Small intestine
Colon
Rectum
Liver
Gallbladder
Pancreas
Kidney
Urinary bladder
Testis
Epididymis
Seminal vesicle
Prostate
Vagina
Ovary
Fallopian tube
Endometrium
Cervix
Placenta
Breast
Heart muscle
Smooth muscle
Skeletal muscle
Adipose tissue
Skin
Appendix
Spleen
Lymph node
Tonsil
Bone marrow
Thymus

B

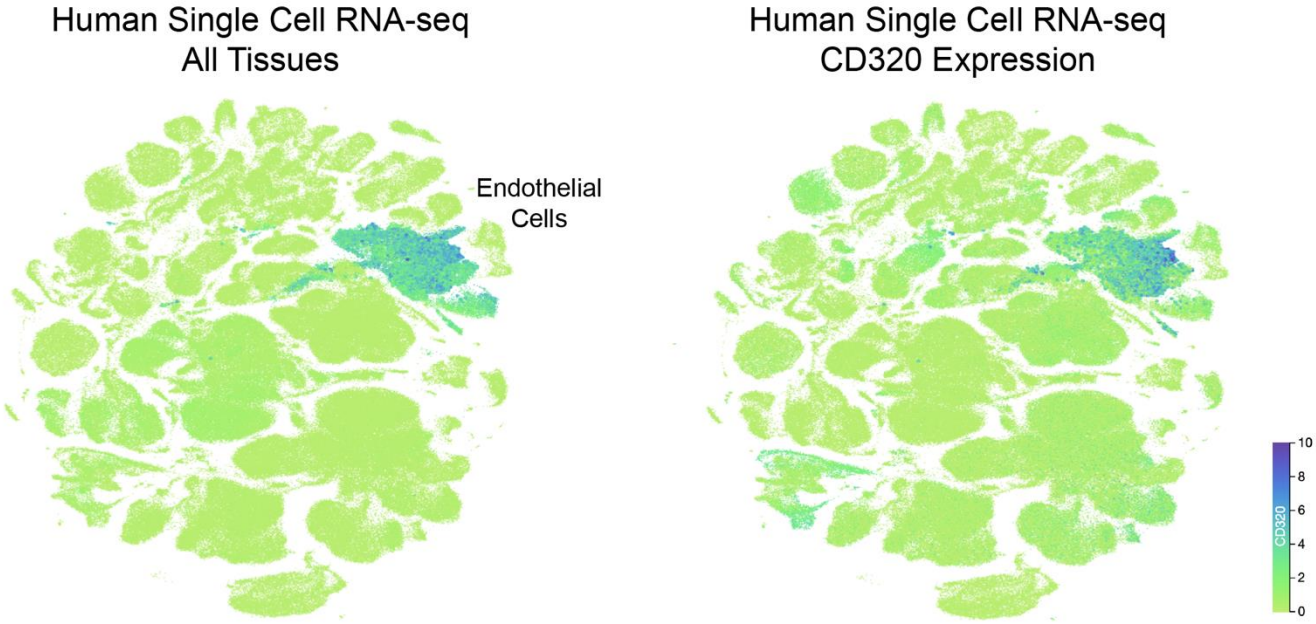
Human Single Cell RNA-seq
All Tissues
Endothelial
Cells
Human Single Cell RNA-seq
CD320 Expression
CD320
10
8
6
4
2
0

C

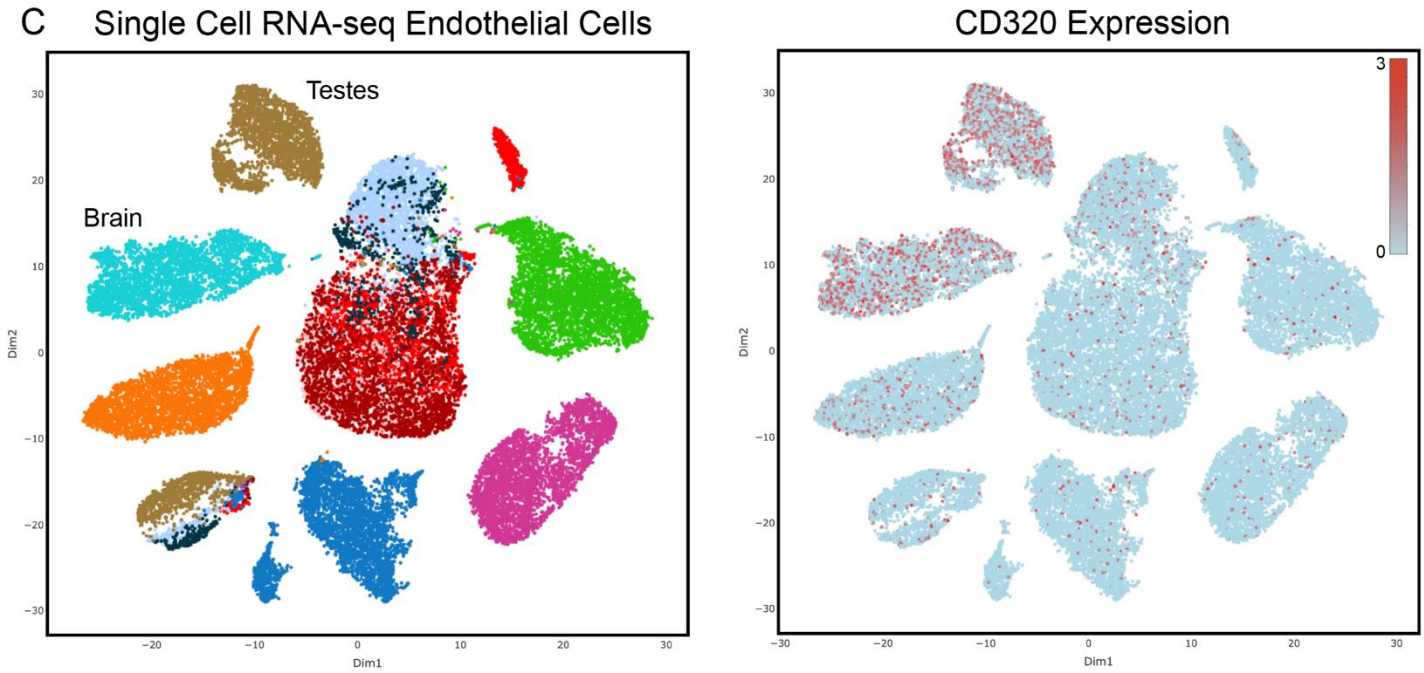
Single Cell RNA-seq Endothelial Cells
Testes
Brain
Dim2
Dim1
CD320 Expression
3
0
Dim2
Dim1

Fig. S2. *CD320* expression in human tissues and single cells.
(**A**) *CD320* expression in multiple human tissues, as measured by bulk RNA-sequencing from the Human Protein Atlas. (**B**) *CD320* expression in multiple human tissues, as measured by single-cell RNA-sequencing from the Tabula Sapiens project (*17*). (**C**) *CD320* expression in endothelial cells from multiple human tissues, as measured by single-cell RNA-sequencing from the EC database (*18*).

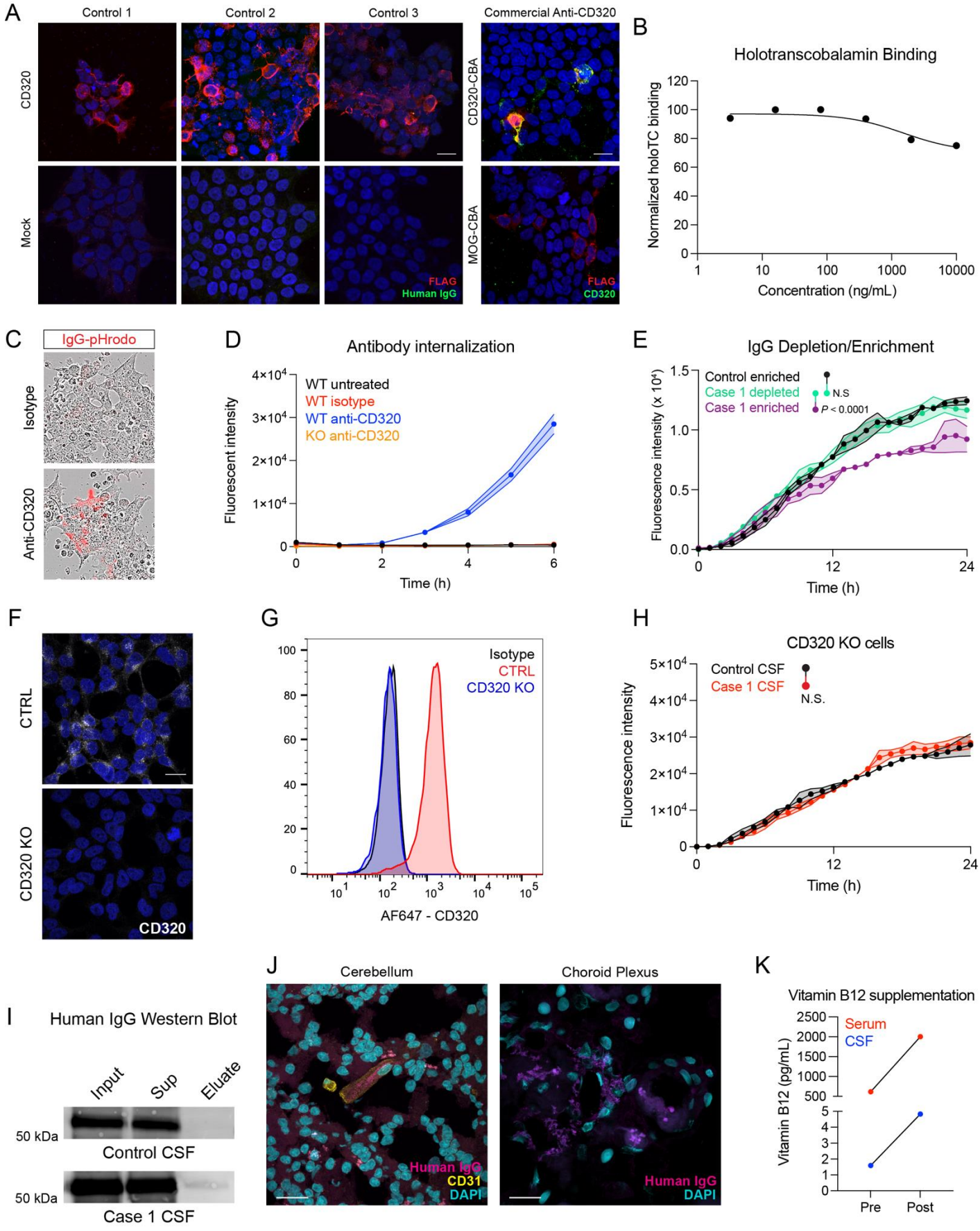
A
Control 1
Control 2
Control 3
Commercial Anti-CD320
CD320
Mock
CD320-CBA
MOG-CBA
FLAG
Human IgG
FLAG
CD320
B
Holotranscobalamin Binding
Normalized holoTC binding
Concentration (ng/mL)
C
IgG-pHrodo
Isotype
Anti-CD320
D
Antibody internalization
Fluorescent intensity
WT untreated
WT isotype
WT anti-CD320
KO anti-CD320
Time (h)
E
IgG Depletion/Enrichment
Control enriched
Case 1 depleted
Case 1 enriched
N.S
P < 0.0001
Fluorescence intensity (x 10⁴)
Time (h)
F
CTRL
CD320 KO
CD320
G
Isotype
CTRL
CD320 KO
AF647 - CD320
H
CD320 KO cells
Control CSF
Case 1 CSF
N.S.
Fluorescence intensity
Time (h)
I
Human IgG Western Blot
Input
Sup
Eluate
50 kDa
Control CSF
50 kDa
Case 1 CSF
J
Cerebellum
Choroid Plexus
Human IgG
CD31
DAPI
Human IgG
DAPI
K
Vitamin B12 supplementation
Serum
CSF
Vitamin B12 (pg/mL)
Pre
Post

Fig. S3. Immunoreactivity and mechanism of anti-CD320.
(**A**) Immunoreactivity of healthy control CSF IgG (green) in HEK293T cells overexpressing FLAG-tagged CD320 (red) (scale bar = 20 microns). (**B**) Dose-response of commercial anti-CD320 on holotranscobalamin binding to the surface of HEK293T cells. (**C**) Representative images of antibody internalization in cells treated with a commercial anti-CD320 antibody or an isotype control antibody. (**D**) Internalization of a commercial anti-CD320 or isotype control antibody in wild type or CD320 KO HEK293T cells (N=3, mean +/- standard error). (**E**) Holotranscobalamin uptake in HEK293T cells treated with IgG-enriched control CSF (black), IgG-enriched case 1 CSF (magenta), or IgG-depleted case 1 CSF (green) (N=3, paired one-way ANOVA with Tukey's multiplicity correction, mean +/- standard error). (**F**) Immunocytochemical staining of control and CD320 KO HEK293T cells with a commercial CD320 antibody (scale bar, 20 microns). (**G**) Flow cytometric quantification of CD320 expression on control and CD320 KO HEK293T cells. (**H**) Holotranscobalamin uptake in CD320 KO HEK293T cells treated with control (black) or case 1 (red) CSF (N=3, paired one-way ANOVA with Tukey's multiplicity correction, mean +/- standard error). (**I**) Western blot for human IgG from input, supernatant, and eluate of an antigen-specific affinity purification of control (top) or patient (bottom) CSF. (**J**) Staining of human cerebellum and choroid plexus tissue with patient immunoglobulin (magenta) and the endothelial marker, CD31 (yellow) (scale bar = 20 microns). (**K**) Vitamin B12 concentration in case 1 serum (red) and CSF (blue) pre- and post-B12 supplementation.

A

CLUSTAL O(1.2.4) multiple sequence alignment

```
clone_1_HC    EVQLVESGGGFVKPGGSLRLSCAASGFTFSDAWMTWVRQAPGKGLEWVGHIKTRSEGEKT  60
clone_2_HC    EVQLVESGGGFVKPGGSLRLSCAASGFTFSDAWMTWVRQAPGKGLEWVGHIKTRSEGEKT  60
clone_3_HC    EVQLVESGGGFVKPGGSLRLSCAASGFTFSDAWMTWVRQAPGKGLEWVGHIKTRSEGEKT  60
clone_4_HC    EVQLVESGGGFVKPGGSLRLSCAASGFTFSDAWMTWVRQAPGKGLEWVGHIKTRSEGEKT  60
clone_5_HC    EVQLVESGGGFVKPGGSLRLSCAASGFTFSDAWMTWVRQAPGKGLEWVGHIKTRSEGEKT  60

clone_1_HC    DYNTPVKGRFTISRDDSRDTVYLEMTSLRTEDTAVYFCLCDLDYWGQGTLVSVSS  115
clone_2_HC    DYNTPVKGRFTISRDDSRDTVYLEMTSLRTEDTAVYFCLCDLDYWGQGTLVSVSS  115
clone_3_HC    DYNTPVKGRFTISRDDSRDTVYLEMTSLRTEDTAVYFCLCDLDYWGQGTLVSVSS  115
clone_4_HC    DYNTPVKGRFTISRDDSRDTVYLEMTSLRTEDTAVYFCLCDLDYWGQGTLVSVSS  115
clone_5_HC    DYNTPVKGRFTISRDDSRDTVYLEMTSLRTEDTAVYFCLCDLDYWGQGTLVSVSS  115

clone_1_LC    DIQMTQSPSSLSASIGDRVTLTCRASQGIHKYLAWYQQKPGKAPKSLIYEASILQTWVPS  60
clone_2_LC    DIQMTQSPSSLSASIGDRVTLTCRASQGIHKYLAWYQQKPGKAPKSLIYEASILQTWVPS  60
clone_3_LC    DIQMTQSPSSLSASIGDRVTLTCRASQGIHKYLAWYQQKPGKAPKSLIYEASILQTWVPS  60
clone_4_LC    DIQMTQSPSSLSASIGDRVTLTCRASQGIHKYLAWYQQKPGKAPKSLIYEASILQTWVPS  60
clone_5_LC    DIQMTQSPSSLSASIGDRVTLTCRASQGIHKYLAWYQQKPGKAPKSLIYEASILQTWVPS  60

clone_1_LC    KFNGSGSGTEFTLTINSLQPEDFATYYCQQYTNFPFTFGPGTKVDFK  107
clone_2_LC    KFNGSGSGTEFTLTINSLQPEDFATYYCQQYTNFPFTFGPGTKVDFK  107
clone_3_LC    KFNGSGSGTEFTLTINSLQPEDFATYYCQQYTNFPFTFGPGTKVDFK  107
clone_4_LC    KFNGSGSGTEFTLTINSLQPEDFATYYCQQYTNFPFTFGPGTKVDFK  107
clone_5_LC    KFNGSGSGTEFTLTINSLQPEDFATYYCQQYTNFPFTFGPGTKVDFK  107
```

B

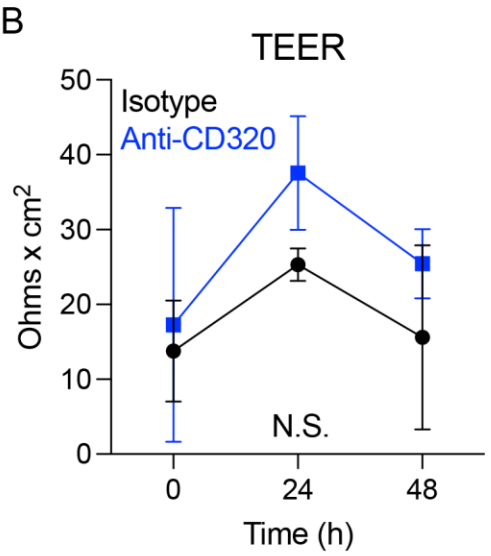

Fig. S4. Characterization of a patient-derived monoclonal autoantibody.
(**A**) Multiple sequence alignment of heavy chain and light chain variable regions of all 5 CD320-specific clones. (**B**) Trans-endothelial electrical resistance (TEER) measurements of iPSC-derived human endothelial transwell monolayers treated with isotype control (black) or anti-CD320 (blue). Measurements were acquired on day 4 after plating at time of treatment (T=0) and every 24 hours after treatment (N=3, two-way ANOVA; mean +/- standard deviation).

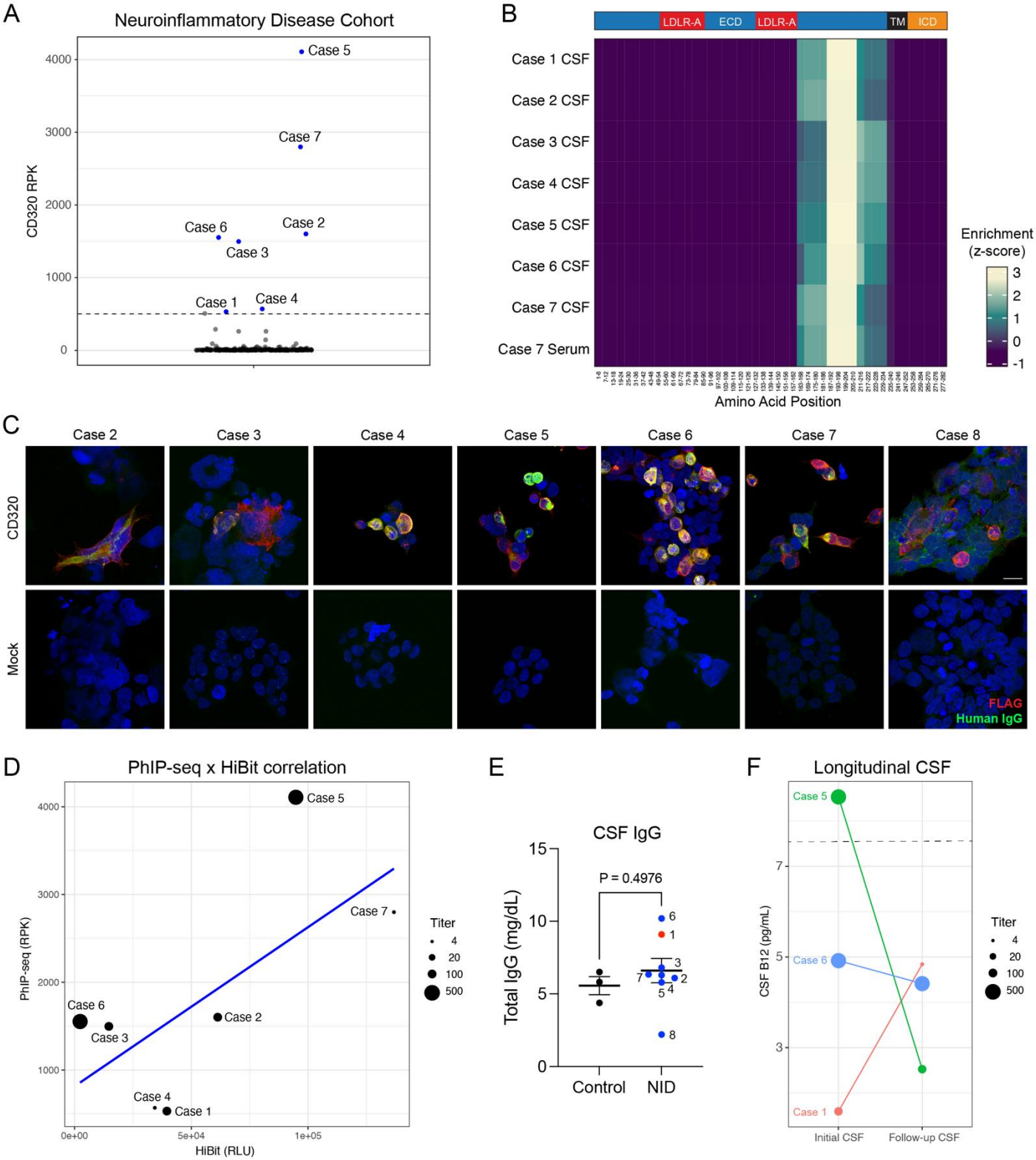
A
Neuroinflammatory Disease Cohort
CD320 RPK
Case 5
Case 7
Case 6
Case 2
Case 3
Case 1
Case 4
B
LDLR-A
ECD
LDLR-A
TM
ICD
Case 1 CSF
Case 2 CSF
Case 3 CSF
Case 4 CSF
Case 5 CSF
Case 6 CSF
Case 7 CSF
Case 7 Serum
Amino Acid Position
Enrichment (z-score)
C
Case 2
Case 3
Case 4
Case 5
Case 6
Case 7
Case 8
CD320
Mock
FLAG
Human IgG
D
PhIP-seq x HiBit correlation
PhIP-seq (RPK)
HiBit (RLU)
Titer
E
CSF IgG
Total IgG (mg/dL)
P = 0.4976
Control
NID
F
Longitudinal CSF
CSF B12 (pg/mL)
Initial CSF
Follow-up CSF
Titer

Fig. S5. Characterization of additional anti-CD320 seropositive patients.
(**A**) CD320 enrichment from PhIP-seq experiments on 254 CSF samples from a neuroinflammatory disease cohort. Labeled samples exhibit CD320 enrichment equal to or greater than CD320 enrichment in the index patient (dotted line). Enrichment was quantified as sequencing reads per 100,000 (RPK) to account for differences in sequencing depth between samples. (**B**) Epitope map of CD320 peptides aligned to the full-length gene (coverage is divided into five amino acid bins). (**C**) Immunoreactivity of CSF IgG (green) for human cells overexpressing FLAG-tagged CD320 (red). Nuclei are stained blue with DAPI (scale bar, 20 microns). (**D**) Correlation between PhIP-seq, HiBit measurements of autoantibody target enrichment, and autoantibody titer as determined by cell-based assay. (**E**) Total IgG concentrations in control CSF and case CSF (two-sided t-test; mean +/- standard error). (**F**) CSF autoantibody titer and corresponding CSF B12 concentrations in three patients for whom longitudinal spinal fluid samples were available.

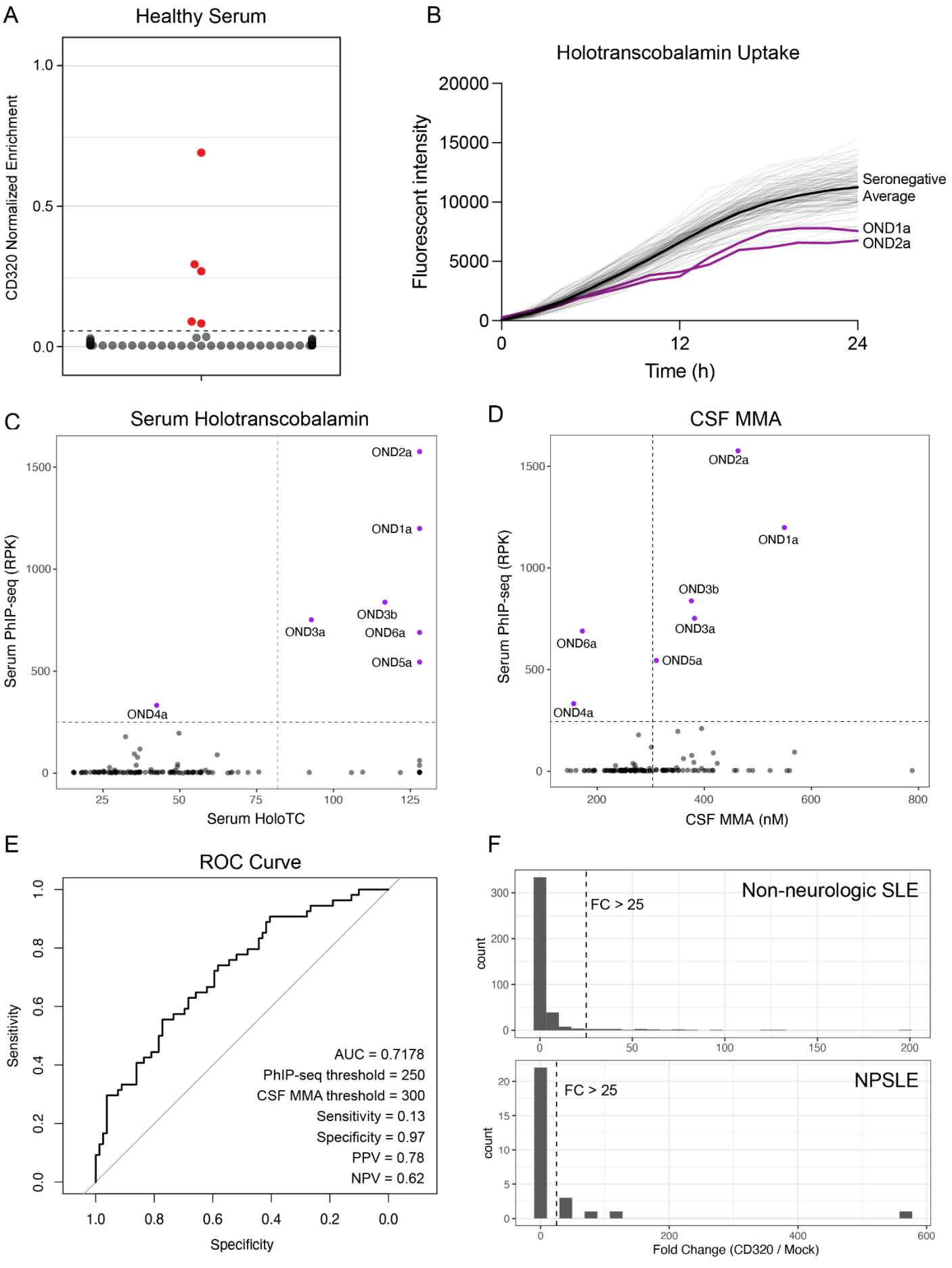
A
Healthy Serum
CD320 Normalized Enrichment
1.0
0.5
0.0
B
Holotranscobalamin Uptake
Fluorescent intensity
20000
15000
10000
5000
0
0
12
24
Time (h)
Seronegative Average
OND1a
OND2a
C
Serum Holotranscobalamin
Serum PhIP-seq (RPK)
1500
1000
500
0
25
50
75
100
125
Serum HoloTC
OND2a
OND1a
OND3b
OND3a
OND6a
OND5a
OND4a
D
CSF MMA
Serum PhIP-seq (RPK)
1500
1000
500
0
200
400
600
800
CSF MMA (nM)
OND2a
OND1a
OND3b
OND3a
OND6a
OND5a
OND4a
E
ROC Curve
Sensitivity
1.0
0.8
0.6
0.4
0.2
0.0
1.0
0.8
0.6
0.4
0.2
0.0
Specificity
AUC = 0.7178
PhIP-seq threshold = 250
CSF MMA threshold = 300
Sensitivity = 0.13
Specificity = 0.97
PPV = 0.78
NPV = 0.62
F
Non-neurologic SLE
FC > 25
count
300
200
100
0
0
50
100
150
200
NPSLE
FC > 25
count
20
15
10
5
0
0
200
400
600
Fold Change (CD320 / Mock)

Fig. S6. Detection of anti-CD320 in healthy controls and patients with multiple sclerosis or other neurologic diseases.
(**A**) Normalized bioluminescent signal from immunoprecipitation of a tagged CD320 peptide after incubation with serum from 84 healthy controls. The dotted line corresponds to a CD320 enrichment threshold set using CSF from the index patient. (**B**) Holotranscobalamin uptake by HEK293T cells treated with CSF from 132 patients with multiple sclerosis (MS) or other neurologic diseases (ONDs). Holotranscobalamin uptake in cells treated with CSF from the two cases with the highest intrathecal anti-CD320 enrichment is indicated by purple lines, and the average effect for CSF from all seronegative patients is indicated by the black line. (**C**) Serum holotranscobalamin concentration vs serum anti-CD320 enrichment in patients with MS or ONDs. (**D**) CSF MMA concentration vs serum anti-CD320 enrichment in patients with MS or ONDs. (**E**) Receiver operator characteristic (ROC) curve showing the performance of serum anti-CD320 seropositivity for predicting a high CSF MMA concentration (**F**) Histograms of CD320 enrichment (fold change over mock) in non-neurologic SLE (top) and NPSLE (bottom). Dashed line shows a fold-change cutoff of 25, above which samples are considered seropositive.

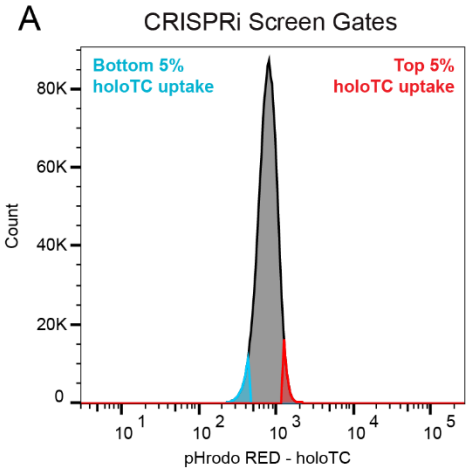
A
CRISPRi Screen Gates
Bottom 5%
holoTC uptake
Top 5%
holoTC uptake
Count
80K
60K
40K
20K
0
10 1
10 2
10 3
10 4
10 5
pHrodo RED - holoTC

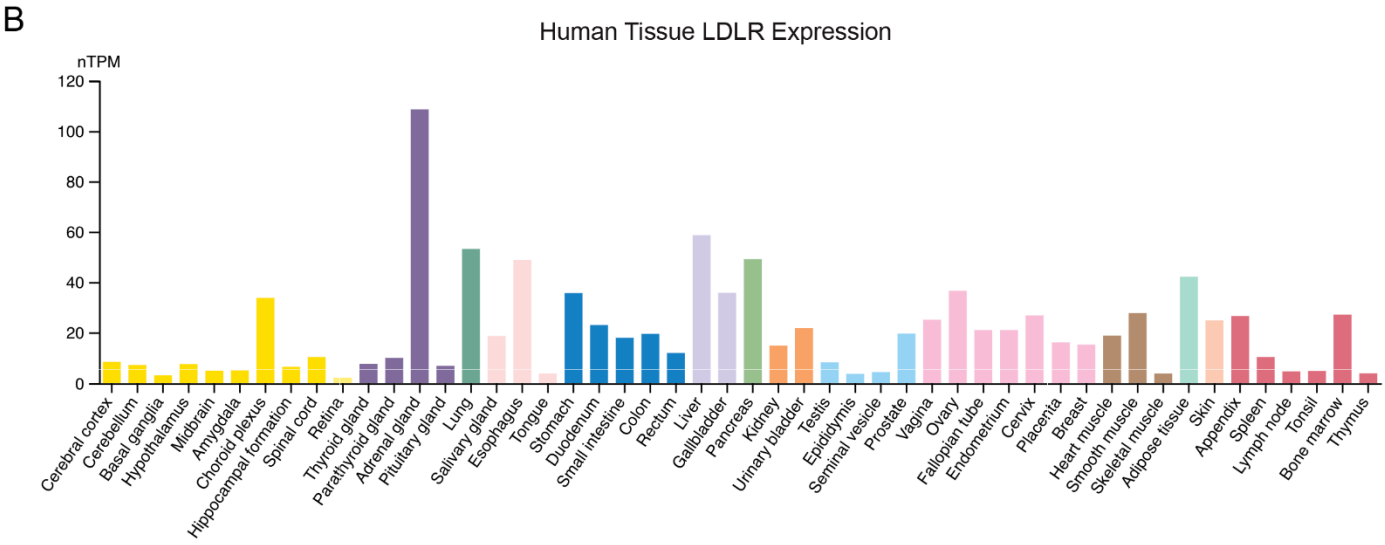
B
Human Tissue LDLR Expression
nTPM
120
100
80
60
40
20
0
Cerebral cortex
Cerebellum
Basal ganglia
Hypothalamus
Midbrain
Amygdala
Choroid plexus
Hippocampal formation
Spinal cord
Retina
Thyroid gland
Parathyroid gland
Adrenal gland
Pituitary gland
Lung
Salivary gland
Esophagus
Tongue
Stomach
Duodenum
Small intestine
Colon
Rectum
Liver
Gallbladder
Pancreas
Kidney
Urinary bladder
Testis
Epididymis
Seminal vesicle
Prostate
Vagina
Ovary
Fallopian tube
Endometrium
Cervix
Placenta
Breast
Heart muscle
Smooth muscle
Skeletal muscle
Adipose tissue
Skin
Appendix
Spleen
Lymph node
Tonsil
Bone marrow
Thymus

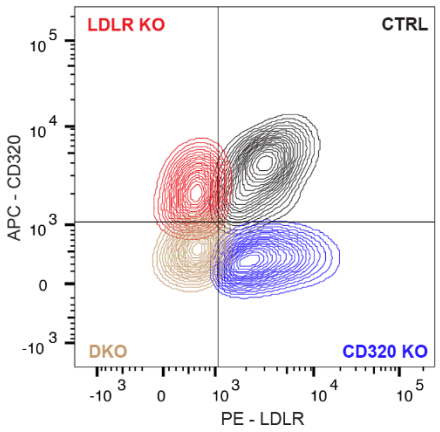
C
HEK293
LDLR KO
CTRL
DKO
CD320 KO
APC - CD320
PE - LDLR

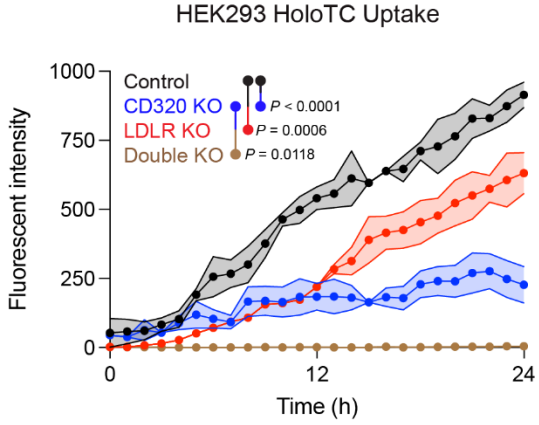
D
HEK293 HoloTC Uptake
Control
CD320 KO
LDLR KO
Double KO
P < 0.0001
P = 0.0006
P = 0.0118
Fluorescent intensity
1000
750
500
250
0
0
12
24
Time (h)

Fig. S7. Validation of CRISPRi Screen Hits.
(**A**) Gating strategy for the CRISPRi screen, wherein K562 library cells with the top 5% (red) or bottom 5% (blue) of internalized holotranscobalamin (represented by pHrodo RED signal) were sorted by FACS. A total of 15 million cells of each population were sorted from 300 million total library cells, each in technical duplicate. (**B**) *LDLR* expression in multiple human tissues, as measured by bulk RNA-sequencing from the Human Protein Atlas. (**C**) Flow cytometry plots of control (black), CD320 KO (blue), LDLR KO (red), and double KO (brown) HEK293 cells. (**D**) Holotranscobalamin uptake by control (black), CD320 KO (blue), LDLR KO (red), or double KO (brown) HEK293 cells (N=3, one-way ANOVA with Tukey's multiplicity correction, mean +/- standard error).

A

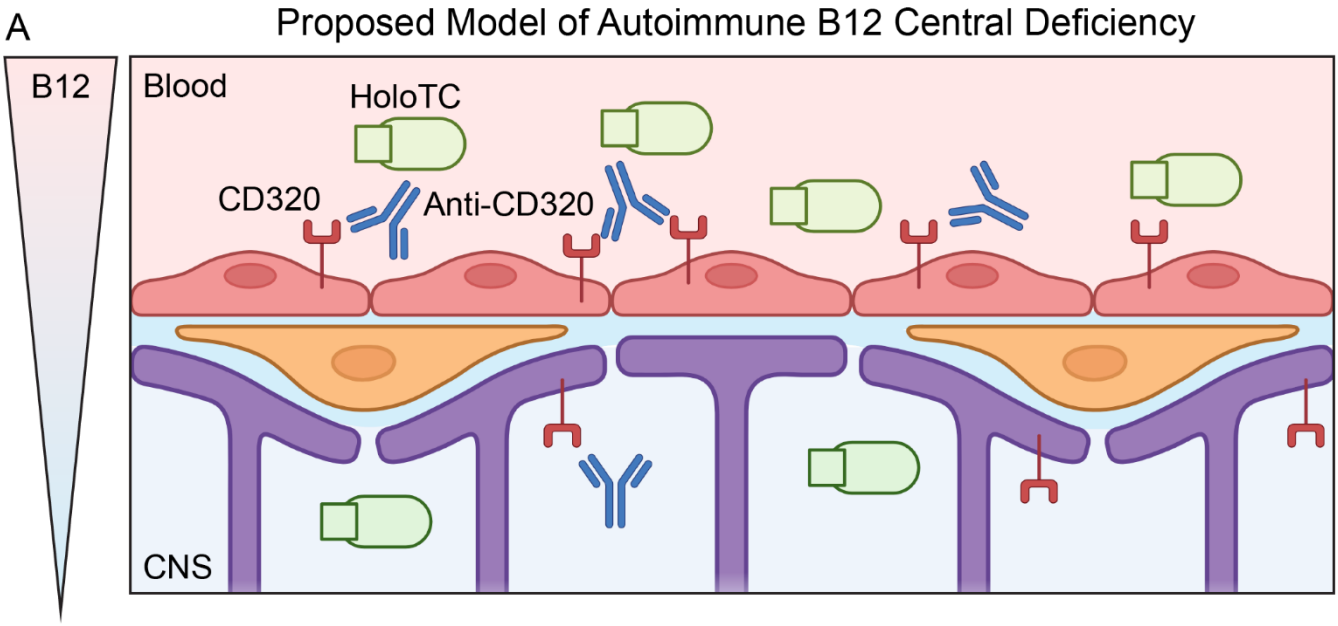
Proposed Model of Autoimmune B12 Central Deficiency
B12
Blood
HoloTC
CD320
Anti-CD320
CNS

B

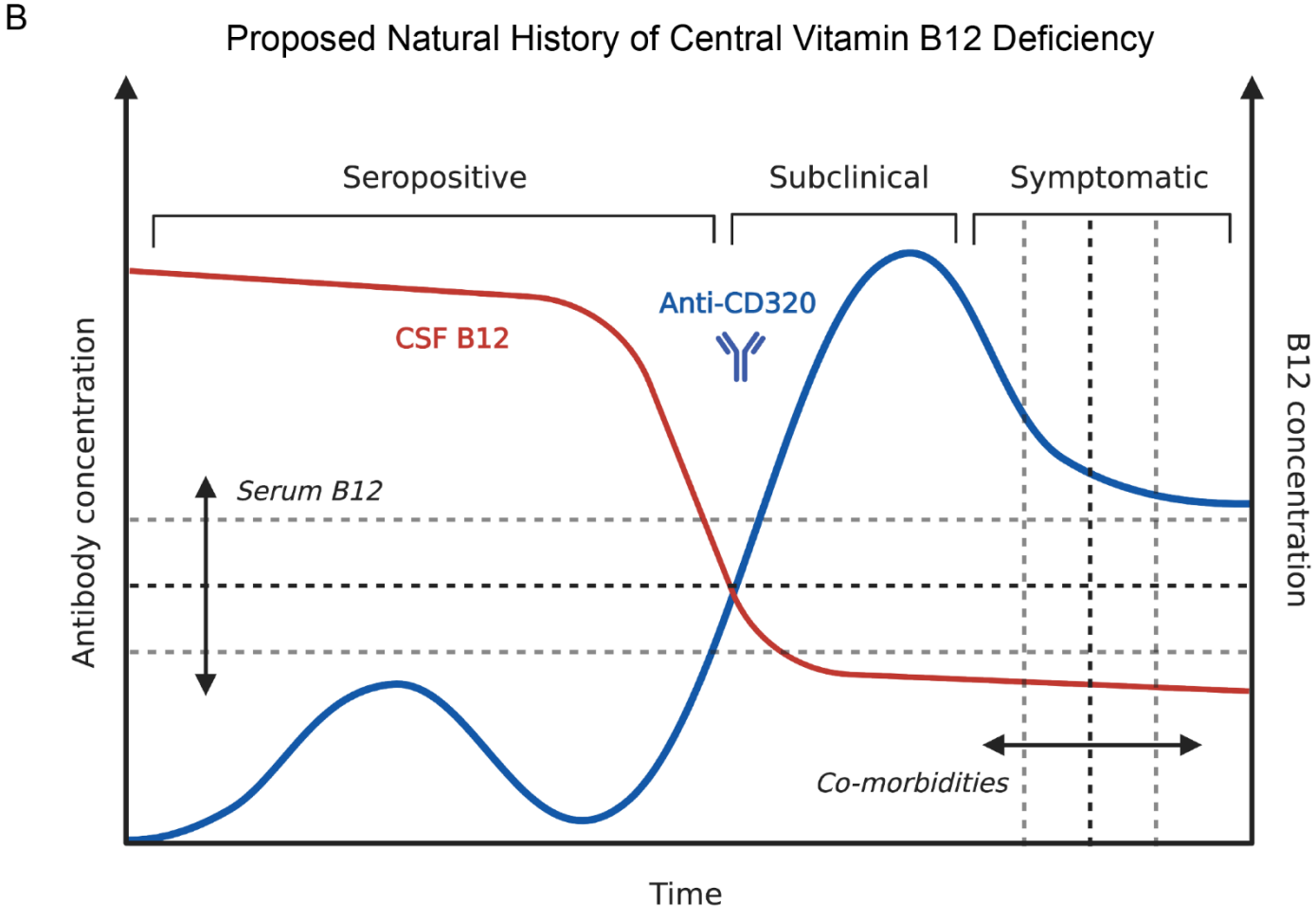
Proposed Natural History of Central Vitamin B12 Deficiency
Seropositive
Subclinical
Symptomatic
CSF B12
Anti-CD320
Serum B12
Co-morbidities
Antibody concentration
B12 concentration
Time

Fig. S8. Proposed model of anti-CD320 mechanism and natural history of disease.
(**A**) Proposed model of anti-CD320 mediated impairment of vitamin B12 transport across the blood-brain barrier. Autoantibodies in the blood impair the uptake function of CD320 on endothelial cells, possibly via internalization and depletion from the luminal cell surface. Holotranscobalamin (holoTC) must cross multiple cellular membranes on its journey to the CSF, including those of endothelial cell (red), pericyte (orange), and astrocyte (purple). Anti-CD320 in the CNS may interfere with uptake of holotranscobalamin by metabolically demanding cell types (neurons, oligodendrocytes), causing neurologic sequelae. These effects may depend on antibody titer, the duration of antibody seropositivity, and host vulnerability. (**B**) Proposed natural history of central vitamin B12 deficiency, divided into three stages of disease (seropositive without clinical symptoms or metabolic signs, subclinical without clinical symptoms but with metabolic signs, and symptomatic with clinical symptoms and metabolic signs). The transition from seropositive to subclinical central B12 deficiency may depend on serum B12 concentration and antibody titer. The transition from subclinical to symptomatic may depend on the degree and duration of seropositivity (area under the curve) and underlying comorbidities predisposing to neurologic frailty. Figure created with BioRender.com.

Table S1. Laboratory test results for Case 1.

Test	2014	2018	Reference
Vitamin D	31.4		10-75 pg/mL
Vitamin E	13.1		4.6-17.8 mg/L
Ferritin	328		11-307 ng/mL
Vitamin B12	614		180-914 pg/mL
MMA (methylmalonic acid)	233		0-378 nmol/L
Hemoglobin	11.8		12-15 g/dL
MCV (mean corpuscular volume)	85.5		78-100 fL
Platelets	96		150-400 k/uL
TSH (thyroid stimulating hormone)	0.75		0.34-3.5 ulU/mL
ANA (anti-nuclear antibody)	1:1280 (mixed)		<1:80
RPR (rapid plasma regain)	Non-reactive		
Copper	95		72-166 ug/dL
CSF glucose	134		40-70 mg/dL
IgG index	0.6		0-0.7
OCBs (oligoclonal bands)	0		0-1
CSF protein	54		15-45 mg/dL
CSF red blood cells	2		0
CSF white blood cells	2		0-5
CSF VDRL (venereal disease research laboratory test)	Non-reactive		
Lyme IgG	negative		
Lyme IgM	negative		
HIV 1/2 Ab	negative		
HCV Ab	negative		
HBV Ag	negative		
HBV surface Ab	positive		
Quantiferon gold	negative		
dsDNA antibody	129		<30 IU/mL
C3	96		71-159 mg/dL
C4	12		13-30 mg/dL
GAD-65 Ab	negative		
MOG IgG		negative	
SSA/SSB	negative		
SM antibody	negative		
RNP antibody	negative		

ANCA	negative		
Paraneoplastic Panel			
ANNA-1	negative		
ANNA-2	negative		
ANNA-3	negative		
AGNA-1	negative		
PCA-1	negative		
PCA-2	negative		
PCA-Tr	negative		
CRMP-5	negative		
Striated muscle	negative		
P/Q-type Ca channel	negative		
N-type Ca channel	negative		
AChR	negative		
VGK channel	negative		
NMO/AQP4	negative		
IgG4	29		1-123 mg/dL
TPO ab	negative		
TG ab	negative		
Anti-Cardiolipin IgG	81		0-14 U/mL
Anti-Cardiolipin IgM	80		0-12 U/mL
B2-glycoprotein IgG	36		<21
B2-glycoprotein IgM	>130		<21
RVVT (Russel viper venom time)	103		0-55.1 sec
HIT (heparin-induced thrombocytopenia) antibody	positive		
ESR (erythrocyte sedimentation rate)	66		0-33mm/hr
CRP (C-reactive protein)	37.4		<6.3 mg/L
FTA-ABS (fluorescent treponemal antibody antibody-absorption)	negative		
Coccidioides Ab	negative		

Table S2. Gene and peptide-level counts for phage display.

Gene	Patient 1_REP1	Patient 1_REP2	CTRL_ REP1	CTRL_ REP2	CTRL_ REP3	meanFC	FDR
SUN1	6385.65025	2802.179481	3.1442247	1.4985302	6.3552737	1102.7134	0.0010749
CD320	623.7213461	440.9736431	0	0	1.3175567	566.81821	0.0011220
ALX4	345.0617519	293.3509147	0.1654855	0.0788700	1.9375834	260.08551	0.0014768
PLAGL2	204.1543657	228.633353	0	0	0	432.78771	0.0014768
PRRX2	102.9018317	130.8749754	0.0827427	0	0.3100133	185.26698	0.0095159
LRRFIP1	3653.337712	2434.714076	15.224667	60.020080	53.244793	70.252403	0.0098385
ZBTB21	1225.14132	171.5697419	1.7375979	11.830502	2.4026034	119.91884	0.0098385
SMTNL1	336.8869722	11.06412646	0	0	0	347.95109	0.0174349
SUGT1	47.68621467	67.97617424	0	0	0	115.66238	0.0252697
GRM2	644.1582953	707.1189318	31.773218	8.1236113	6.0452604	42.723999	0.0288232
MPZL3	25.81509366	129.3593416	0	0.1577400	0.7750333	95.677489	0.0288232
ANKIB1	66.90411772	35.0869216	0	0.6309601	1.0850467	47.570346	0.0428992
C12orf45	74.07497707	26.37202746	0	0	0	100.44700	0.0428992

Peptide	Gene	Sequence	FC	FDR
gi|195972890|ref|NP_001124437.1	SUN1	PRMSRRSLRLATTACTLGDGEAVGADSGTSSAVSLKNRAARTTKQRRST	6530.91	0.0022
gi|284925167|ref|NP_001165416.1	SUN1	SYSSDALDFETEHKLDPVFDSPRMSRRSLRLATTACTLGDGEAVGADSG	796.08	0.0037
gi|767950082|ref|XP_011533022.1	TDRP	ADPEDTVGGHPSWSGWEDDAKGSTKYTSLASSANSSRWSLRAAGRLSLK	1728.48	0.0052
gi|55743092|ref|NP_068745.2	ALX4	RASSDLPSPLEKADSESNKGKKRRNRTTFTSYQLEELEKVFQKTHYPDV	632.96	0.0063
gi|578805170|ref|XP_006712910.1	LRRFIP1	HESPSQDISDACEAESTERCEMSEHPSQTVRKALDSNSLENDDLSAPGR	4527.18	0.0063
gi|740086846|ref|NP_001290203.1	ACLY	MGAGKSPAGPGQKPDPGKLPAAGVLRILRGSSGLWKKRRARTSAETGRA	680.61	0.0063
gi|767923065|ref|XP_011531938.1	GRM2	GCLFAPKLHIILFQPQKNVVSHRAPTSRFGSAAARASSSLGQGSGSQFV	798.49	0.0063
gi|116812638|ref|NP_778250.2	TDRP	EDDAKGSTKYTSLASSANSSRWSLRAAGRLVSIRRQSKGHLTDSPEEAE	3896.72	0.01359
gi|118498345|ref|NP_008816.3	ZFHX3	PSPTKPKTKPTWRCEVCDYETNVARNLRIHMTSEKHMHNMMLLQQNMTQ	370.92	0.01438
gi|259906403|ref|NP_001159367.1	CD320	DELGCGTNEILPEGDATTMGPPVTLESVTSLRNATTMGPPVTLESVPSV	636.46	0.01438
gi|768004140|ref|XP_011526619.1	LPPR3	EGAPRPVAREKTSLGSLKRASVDVDLLAPRSPMAKENMVTFSHTLPRAS	848.05	0.01438
gi|768020854|ref|XP_011527889.1	ZBTB21	SSQGSSSVSSDAPGNVLCALSQKSSLKDCSEKTALDDRPQVLQPHRLRS	1380.30	0.01438
gi|767923088|ref|XP_011531949.1	GRM2	VSLSGSVVLGCLFAPKLHIILFQPQKNVVSHRAPTSRFGSAAARASSSL	344.28	0.01498
gi|259906403|ref|NP_001159367.1	CD320	LESVTSLRNATTMGPPVTLESVPSVGNATSSSAGDQSGSPTAYGVIAAA	417.04	0.02155
gi|530418157|ref|XP_005260493.1	PLAGL2	FSNGEKLRPHSLPQPEQRPYSCPQLHCGKAFASKYKLYRHMATHSAQKP	432.18	0.02155

Table S3. Additional clinical information for Cases 1-8.

	Case 1	Case 2	Case 3	Case 4	Case 5	Case 6	Case 7	Case 8
Labs								
B12	614	567			803	573		745
MMA	.23				**0.63**	0.1		0.18
Homocysteine		6.5				10		
ANA			<1:80		1:40 (speckled)			<1:80
dsDNA	positive				negative			
SSA/SSB	negative		<0.2 U		negative			negative
Rheumatoid Factor			<0.2 U		negative			
Anti-phospholipid antibodies	positive	negative						
Serum IgG (mg/dL)	2210				1470			639
CSF IgG (mg/dL)	9.1 (pre-treatment); 9.2 (post-treatment)	6.1	6.8	6.3	5.8	10.2	6.3	2.2
IgG index	0.6				0.8			0.6
Imaging								
MRI brain	bilateral symmetric T2-weighted hyperintensities in the superior cerebellar peduncles, midbrain tegmentum, dentate nuclei, chief sensory nuclei of cranial nerve V, and rubrospinal tracts persist, with contrast enhancement		bilateral superior cerebellar peduncle T2-hyperintensity without enhancement; resolved after steroids		scattered foci of bilateral, right greater than left, T2/FLAIR hyperintensities insula, subinsular white matter, and hippocampi with two small foci of enhancement, nonspecific, but consistent with sequela of meningoencephalitis given the history, which may be inflammatory or infectious. No areas of reduced diffusion.	multifocal white matter T2 hyperintensities		no intracranial abnormality to explain the patient's weakness

MRI C/Tspine	normal	normal	normal		Multilevel degenerative changes of the spine without severe canal narrowing.	normal		Abnormal cord signal within the dorsal and lateral columns of the cervical cord, and likely within the conus medullaris. The thoracic cord was not well evaluated. Findings are compatible with subacute combined degeneration and can be seen in the context of vitamin B12 or copper deficiency as well as due to inflammatory/ post-infectious etiologies.
MRI L-spine								
Medications								
Steroids	IVSM	IVSM	prednisone		prednisone	none		IVSM
B12 supplement	1000mcg IM weekly then 2000mcg PO daily	none	none		none	none		2000mcg PO daily
Other immuno-suppression	HCQ	IVIG	Adalimumab/ certolizumab for arthritis		Anakinra	prior rituximab for MALToma; prior R-CHOP for NHL		IVIG/PLEX/ rituximab

Table S4. Case vignettes.

Case 2: 51-year-old male with cognitive decline, ataxia, and psychosis
A previously healthy 51-year-old male presented with 4 weeks of increasing confusion, weakness, gait disorder, and hallucinations. He had recently been traveling internationally and had experienced flu-like symptoms which were resolved at time of admission. A generalized seizure occurred several days into the hospitalization followed by a complicated intensive care unit stay with aspiration pneumonia, pulmonary emboli, and respiratory failure. His brain MRI was unremarkable and CSF showed mild elevation of protein but no pleocytosis. A paraneoplastic antibody panel was negative. Cognitive symptoms and balance returned to near baseline prior to discharge. He returned to work for several weeks, but cognitive and motor symptoms recurred, including multiple falls due to challenges with balance and weakness. He was readmitted to the hospital, again with unremarkable MRI brain, CSF with elevated protein but otherwise normal, negative CSF paraneoplastic and autoimmune encephalopathy panel, negative oligoclonal bands, negative whole body PET scan for malignancy, and negative scrotal ultrasound. EEG showed a single left anterior temporal sharp and slow wave discharge superimposed on a normal posterior dominant rhythm. Neuropsychological testing showed impairments in attention (Trails A: 50 sec.), memory (2/10 on wordlist delayed recall), executive function (could not complete Trails B), language (category fluency: 13 animals in 60 sec.), and MOCA (18/30). Neurological exam was notable for a fine high amplitude action tremor, wide-based gait, startle myoclonus, and frontal release signs including glabellar tap and palmomental reflex. He eventually received 5 days of IV solumedrol and demonstrated remarkable improvement in symptoms. Over the course of the next several months, he was readmitted multiple times for pulse steroids and ultimately started on IVIG every 3 weeks with complete resolution of motor and cognitive symptoms. Repeat MRI brain scans never showed any abnormal signal or enhancement, nor was there any evidence of progressive atrophy when comparing scans. Repeat neuropsychological testing (7 months after the testing above) demonstrated normal cognition (attention: Trails A-20 sec.; memory: 9/10 on wordlist delayed recall; executive function: Trails B-65 sec.; language: category fluency-26 animals in 60 sec.; MOCA-27/30). Tremulousness and gait disorder had also resolved. He remained on IVIG for 3 years and was slowly tapered off with full return to work without cognitive sequelae.
Case 3: 44 year-old male with joint pain, gait impairment, and imbalance
A previously healthy 44-year-old male presented with acute on chronic diffuse musculoskeletal pain and weakness. He reported that symptoms had started about a year prior to presentation, starting subtly and worsening acutely 4 months prior to presentation after 1 week of nasal congestion and diarrhea. Shortly after, he developed migratory joint pain starting in the left hip, then right hip, then right shoulder. Ultimately, the pain involved the large joints, chest, neck and back. He had substantial difficulty rising from a chair and walking short distances in part due to balance issues. He lost weight from baseline weight of 190 to 177 lbs. Initial lumbar puncture showed 69 white blood cells, 9 red blood cells, total protein of 64 mg/dL, normal glucose, and zero oligoclonal bands. Two months after presentation, a brain MRI revealed T2-hyperintesity in the cerebellar peduncles and dorsal brainstem without enhancement. C- and T-spine MRI showed equivocal anterior spinal cord T2-hyperintensity without enhancement. Initial management included prednisone taper with improvement after first dose, then plateauing of improvement. Repeat lumbar puncture showed resolution a WBC <1/µL and protein of 98 mg/dL. Infectious workup was negative except for CSF meta-next generation sequencing positive for *Bacillus infantis* which was felt to be a contaminant. Rheumatology evaluation suggested axial inflammatory arthritis and spondyloarthropathy and the patient started treatment with adalimumab, initially with a good response but developed autoantibodies. He then switched to certolizumab with partial response.
Case 5: 60 year-old male with cognitive decline, bilateral scleral injection, and hearing loss
A previously healthy 60 year-old male presented with subacute progressive cognitive decline, bilateral scleral injection, and hearing loss. One month prior to presentation, he developed leg pain requiring a crutch to walk. A few weeks later, he started displaying odd behaviors including driving the wrong direction in a car, laughing inappropriately, and occasionally speaking unintelligibly. Over the next few weeks, he began to develop headaches. These were intermittent and without meningism. He started to become confused at work and was unable to complete simple tasks. In addition, he developed hearing loss. This prompted presentation to a hospital, where lumbar puncture yielded CSF with a lymphocytic pleocytosis but with a significant percentage of polymorphonuclear cells (WBC 39, Lymph 73%, PMN 26%), elevated protein (80), and a normal glucose (53). His brain MRI demonstrated subtle leptomeningeal enhancement and parenchymal changes in the lentiform nucleus. He was briefly treated with antimicrobials, but these were stopped after two days as it was felt he did not have features consistent with a bacterial meningitis. During his hospital admission, he developed bilateral scleral injection. There was no discharge or gritty sensation of the eyes. He also developed profound hearing loss at this stage and required a whiteboard to communicate. A repeat LP demonstrated a worsening pleocytosis (WBC 120, Lymph 73%, PMN 11%). A broad infectious workup and cytology were negative. He was discharged from the hospital with a walker due ongoing pain and soreness in his lower limbs, and had developed a new bilateral upper extremity action tremor. He was referred to a neuroimmunology specialty clinic where atypical infectious (TB, fungal, VZV), autoimmune (autoimmune encephalitis, sarcoidosis, Vogt-Koyanagi-Harada, Susac's and Cogan's syndrome, systemic vasculitis), and neoplastic

etiologies were considered (lymphoma). Repeat LP demonstrated persistent pleocytosis with an elevated OCB and IgG index. Next generation metagenomic sequencing did not demonstrate an infective cause. CT chest/abdomen/pelvis, testicular ultrasound, and a PET scan did not demonstrate evidence of a malignancy. An encephalopathy panel was also negative for paraneoplastic or autoimmune causes. Ophthalmological review did not demonstrate any evidence of ongoing uveitis. ESR and CRP were elevated.

He was empirically treated with prednisone for presumed autoimmune meningoencephalitis and experienced significant improvement in his mood and mobility. Upon tapering the steroids, he experienced worsening behavioral changes characterized by automatisms of rearranging bathroom items and speaking incoherently. He had a generalized tonic-clonic seizure and re-presented to the hospital. Repeat brain MRI demonstrated interval progression FLAIR hyperintensities and leptomeningeal enhancement. He underwent a brain biopsy that was non-diagnostic and received high dose steroids, rituximab, and IVIG. This suspected relapse of autoimmune meningoencephalitis left him bedbound and non-verbal. A repeat lumbar puncture after discharge demonstrated recurrent pleocytosis, and he was empirically treated with Anakinra given prior failure of steroids and rituximab. Genetic testing revealed a heterozygous mutation in the C5 gene of uncertain significance. He contracted a severe COVID-19 infection and died without a clear diagnosis.

Case 6: 52 year-old male with HIV, cognitive decline, and progressive white matter disease

A 52-year-old male with a history of gastric marginal zone lymphoma, non-Hodgkin's lymphoma, toxoplasma encephalitis, and HIV infection presented with gradual cognitive decline and progressive subcortical white matter lesions. He was diagnosed with gastric marginal zone lymphoma 9 years prior to presentation and treated with a course of rituximab. Four years later, he was diagnosed with non-Hodgkin's lymphoma and treated with cyclophosphamide, doxorubicin, vincristine, prednisone, and rituximab (R-CHOP) and radiation. One year later, he was found to be HIV-positive in the context of biopsy confirmed toxoplasma encephalitis that was successfully treated with pyrimethamine, sulfadiazine, leucovorin, and antiretroviral therapy (ART). Despite ART with suppression of plasma HIV below the limit of detection and a rise in his CD4 T-cell count to >200 cells/μL, he continued to develop new subcortical white matter lesions though there was no mass effect and no enhancement suggesting a process separate from the treated toxoplasma encephalitis.

He continued to exhibit a gradual decline in cognitive function over several years with impairments in memory, executive function, and psychomotor speed predominantly. Serial lumbar punctures were unrevealing for opportunistic infections or evidence of detectable HIV in CSF. A brain biopsy of one of the white matter lesions that developed after toxoplasma encephalitis treatment showed mild astrogliosis and no other inflammatory or infectious features. Despite escalations of ART and continued maintenance toxoplasma encephalitis treatments, he continued to have progressive cognitive decline and worsened global cerebral atrophy with some suggestion of increasing size of existing white matter lesions. Serum vitamin B12, methylmalonic acid, and homocysteine levels consistently remained within normal limits without supplementation.

Case 8: 80 year-old male with progressive numbness and weakness

An 80 year-old male with a history of hypertension and hyperlipidemia contracted COVID-19 and recovered over the course of 2 weeks. One month later, he developed bilateral toe numbness followed by bilateral leg weakness. These symptoms progressed until he developed new bowel and bladder incontinence, prompting urgent imaging which revealed lumbar stenosis for which a laminoforaminotomy was performed. His post-op course was complicated by a pulmonary embolism. On post-op day three, his leg weakness worsened. Total spine imaging revealed dorsal column and lateral corticospinal white matter tract T2 hyperintensity throughout the cervical and thoracic cord. Serum vitamin B12, MMA, and copper were normal. Lumbar puncture yielded CSF with 3 WBCs, 14 RBCs, protein of 41, glucose of 65, normal IgG index, and zero oligoclonal bands. A paraneoplastic antibody panel, AQP4 antibody, and MOG antibody were negative. He was empirically treated with high-dose steroids followed by plasmapheresis due to lack of response for a presumed post-COVID myelitis. He was then treated with rituximab and empiric high dose oral vitamin B12 supplementation despite normal serum levels. Lower extremity motor function and sensory deficits partially recovered.

Table S5. Clinical phenotypes of anti-CD320 positive NPSLE cases.

ID	Clinical history	SLE diagnosis	Aseptic meningitis	Cerebrovascular disease (not otherwise explained by APLS)	Demyelinating syndrome	Movement disorder	Myelopathy (not otherwise explained by AQP4)	Seizure disorders	Acute confusional state	Cognitive dysfunction (moderate or severe)	Severe depression (acute onset)	Psychosis
Case 1	63F w/ ataxia, tremor, scanning speech	x					x			x		
NPSLE_2	46F w/ progressive encephalopathy and psychosis	x								x		x
NPSLE_3	53F w/ cognitive decline	x								x		
NPSLE_4	43F w/ progressive myelopathy, seizures, psychosis	x			x		x	x		x		x
NPSLE_5	Child w/ meningitis and myelopathy	x	x		x		x					
NPSLE_6	35F w/ encephalopathy, psychosis, seizures	x						x		x		x

Table S6. CRISPR screen hits.

Symbol	Combo casTLE Effect	Combo casTLE Score	FDR
MYLIP	4.8	167	1.00E-05
LDLR	-3.7	114	1.00E-05
FECH	4.6	111	1.00E-05
SLC46A3	2.8	102	1.00E-05
VPS4A	4.2	90.8	1.00E-05
CD320	-2.7	72.5	1.00E-05
MEN1	-3.6	58.1	1.00E-05
CAND1	2.4	51.6	1.00E-05
MAP2K3	-2.9	50.9	1.00E-05
PPOX	3.4	44.7	1.00E-05
TSC1	2.9	44.1	1.00E-05
RPTOR	-2.4	42.4	1.00E-05
KLF16	2.6	38.6	1.00E-05
ZC3H13	3.5	37.5	1.00E-05
GFI1B	-2.7	37.2	1.00E-05
PPP2R2A	-2.3	35.4	1.00E-05
MAP3K4	-3.2	35	1.00E-05
NEDD8-MDP1	2.3	32.9	1.00E-05
UROD	4.4	32.1	1.00E-05
TMED10	-3	31.9	1.00E-05
ATP6V1C1	-2.7	31.5	1.00E-05
SHFM1	-2.4	31.2	1.00E-05
STAT5A	1.6	30.2	1.00E-05
PRPF6	2.4	30.2	1.00E-05
ATP6V1G1	-2	29.9	1.00E-05
HSPA14	4.3	29.4	1.00E-05
MARCKSL1	-2.2	28.8	1.00E-05
SF1	1.7	28.7	1.00E-05
AP2B1	-2.1	28.5	1.00E-05
CCND3	3.2	28	1.00E-05
UBA6	1.8	28	1.00E-05
EXOC2	-2.6	27.8	1.00E-05
UBR5	-2.2	27.7	1.00E-05
SEC31B	-2.2	27.6	1.00E-05
LAMTOR3	-1.9	27.4	1.00E-05
TSG101	1.9	27.3	1.00E-05

PPP1R10	-3.3	26.9	1.00E-05
EXOC6	-3.1	26.7	2.00E-05
CHORDC1	-2.2	26.5	3.00E-05
FAM117A	2.6	26.4	3.00E-05
FOXK1	-2.5	26.3	3.00E-05
ALDH18A1	-2	25.8	3.00E-05
ABCE1	2.5	25.8	3.00E-05
COMMD10	2.7	25.4	4.00E-05
MCM10	2.2	25	4.00E-05
ATP6V1A	-1.8	24.9	5.00E-05
RASA3	1.6	24.8	5.00E-05
TMEM261	-3	24.5	6.00E-05
NRF1	-1.5	24.3	6.00E-05
CNPY1	4.4	24.3	6.00E-05
CDC23	2.5	24.3	6.00E-05
SPINK6	-1.9	24.2	6.00E-05
SMARCA5	2.4	24	7.00E-05
FIP1L1	2.5	24	7.00E-05
ZC3H4	-1.6	23.8	9.00E-05
TTI2	-2.9	23.5	0.00012
CNOT3	-2.5	23.4	0.00012
RPL13	2.2	23.4	0.00012
COPZ1	-2.1	22.9	0.00014
NEDD8	2.3	22.9	0.00014
HLA-DOA	-3.4	22.8	0.00014
SNW1	4.7	22.8	0.00014
NUP43	-2	22.6	0.00014
EIF2AK1	-2.7	22.6	0.00014
ZBTB7B	-2.3	22.5	0.00014
PAXBP1	1.7	22.4	0.00014
WDR91	1.7	22.3	0.00015
GCN1L1	2.7	21.9	0.00019

Data file S1. Raw data for figures.